Scientia Iranica, Vol. 12, No. 2, pp 247–254

SCIENTIA IRANICA

Research Note

Transient Laminar Convection Induced by a Line Heat Source: A Numerical Study with Primitive Variables

M.B. Ayani[1], J.A. Esfahani[*], H. Niazmand[1] and A.C.M. Sousa[2]

The present work is addressed to the numerical study of transient laminar natural convection in an open space and induced by a line heat source. The governing equations, full Navier-Stokes and energy equations with primitive variables, are discretized in a staggered grid by a control volume approach. The equations for the fluid and solid (line heat source) phases are solved simultaneously using a segregated technique. Some of the physical and thermo-physical properties of the fluid (air), such as density, thermal conductivity and viscosity, were considered to vary with temperature. The results show that the energy equation reaches the steady state condition more rapidly than the momentum equations. Hence, at that time, the distribution of temperature does not show any change within the accuracy of the solution, while the distribution of the velocity still varies. The steady-state results obtained via the time-marching solution show good agreement with the published steady-state, self-similar results in the vicinity of the centerline of the plume. Also, the steady-state streamlines compare well with the published experimental results.

INTRODUCTION

Two-dimensional laminar natural convection from horizontal cylinders and a line heat source in an infinite fluid space has been extensively investigated analytically, numerically and experimentally.

The first analytical study of steady-state natural convection plumes above a point and a horizontal line heat source was conducted by Zeldovich [1], neglecting the velocity component normal to the symmetry plane of plume. Fujii [2] and Gebhart et al. [3] solved the two-dimensional steady-state boundary layer equations by using a similarity approach. It should be mentioned that even some experimental work, e.g. [4], uses the results of Fujii for comparison and validity assessment.

Brodowicz and Kierkus [4], Forstrom and Sparrow [5], and Schorr and Gebhart [6], studied the steady-state laminar plume arising above electrically heated wires by experimental methods. The steady-state, laminar, free convection induced by a line heat source at low Grashof number was studied by Linan and Kurdymov [7]. The steady-state Navier-Stokes and energy equations were numerically solved in a stream function and vorticity (ψ, ω) form under the Boussinesq assumption. A few numerical studies were conducted to analyze the plume arising from heated horizontal circular cylinders; however, most of the body of prior work was concentrated on the steady-state situation. In what follows, those studies dealing with numerical transient free convection are succinctly reviewed.

Transient, laminar and natural convection from heated wires or horizontal circular cylinders, was studied numerically by Katagiri and Pop [8], Sako et al. [9], Shin and Chang [10] and Wang et al. [11]. In all of these studies, the Navier-Stokes were solved in the (ψ, ω) form and the energy equations with appropriate assumptions. Esfahani and Sousa [12], in a study addressed to the ignition by radiation, used a primitive variable segregated numerical method to analyze the laminar thermal plume up to the ignition threshold.

To the authors' best knowledge, the solution of the full Navier-Stokes and energy equations for a transient laminar plume arising over a heat line source,

1. *Department of Mechanical Engineering, Ferdowsi University of Mashhad, P.O. Box 91775-1111, Mashhad, I.R. Iran.*
*. *Corresponding Author, Department of Mechanical Engineering, Ferdowsi University of Mashhad, P.O. Box 91775-1111, Mashhad, I.R. Iran.*
2. *Department of Mechanical Engineering, University of New Brunswick, P.O. Box 4400, Fredericton, NB, Canada.*

so far, has not been reported in the open literature. In this study, the transient full Navier-Stokes, in the primitive variables and energy equations, are solved by a segregated numerical method [12-14]. The convective-diffusive linkage in this study uses the second order upwind, which, based on different numerical tests, was found to be computationally efficient, also, its artificial viscosity level is lower than that of the first order upwind scheme [15]. The governing equations were discretized for a non-uniform staggered grid and the physical and thermo-physical properties of the fluid, such as density, thermal conductivity and viscosity, were considered to be dependent upon the temperature.

GOVERNING EQUATIONS

The natural convection midplane flow from a horizontal line heat source, assuming the end-effects of the source are negligible, is governed by the continuity equation, two-dimensional Navier-Stokes equations and the energy equation. For simplicity, the shape of the line heat source considered here has a square cross-section, because the size of the line heat source is chosen relatively small and the shape of it has an effect only on the flow adjacent to it. The pattern of the flow depends on the properties of the fluid, the height away from the heat source and the heat input rate. The transition beginning of the flow is characterized by a local Grashof number, based on the heat input rate. This occurred at a flow Grashof number equal to 5×10^8 [16]. Based on the physical configuration shown in Figure 1, the governing equations for laminar flow in the Cartesian coordinate system, take the following form:
Continuity equation:

$$\frac{\partial \rho}{\partial t} + \nabla.(\rho V) = 0, \tag{1}$$

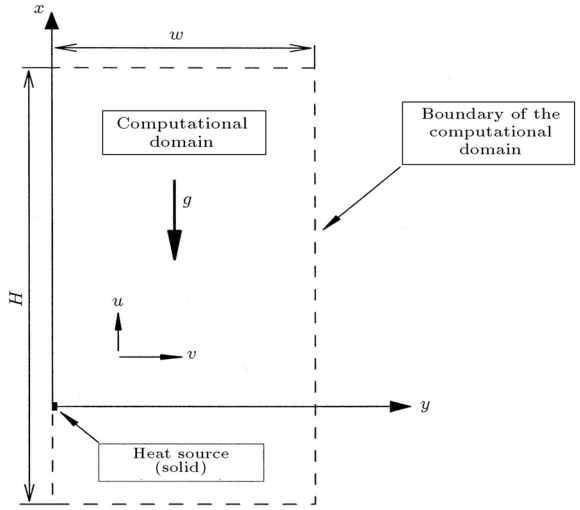

Figure 1. Schematic of the computational domain and the Cartesian coordinate system.

where:

$$V = u\hat{i} + v\hat{j}. \tag{2}$$

Momentum in x direction:

$$\frac{\partial(\rho u)}{\partial t} + \frac{\partial(\rho u^2)}{\partial x} + \frac{\partial(\rho uv)}{\partial y} = X - \frac{\partial p}{\partial x} + \left(\frac{\partial \sigma_x}{\partial x} + \frac{\partial \tau_{yx}}{\partial y}\right). \tag{3}$$

Momentum in y direction:

$$\frac{\partial(\rho v)}{\partial t} + \frac{\partial(\rho uv)}{\partial x} + \frac{\partial(\rho v^2)}{\partial y} = -\frac{\partial p}{\partial y} + \left(\frac{\partial \tau_{xy}}{\partial x} + \frac{\partial \sigma_y}{\partial y}\right), \tag{4}$$

where:

$$\sigma_x = -\frac{2}{3}\mu\nabla.\vec{V} + 2\mu\frac{\partial u}{\partial x},$$

$$\sigma_y = -\frac{2}{3}\mu\nabla.\vec{V} + 2\mu\frac{\partial v}{\partial y},$$

$$\tau_{xy} = \tau_{yx} = \mu\left(\frac{\partial v}{\partial x} + \frac{\partial u}{\partial y}\right). \tag{5}$$

In Equation 3, X is the body force per unit volume in the x direction. The energy equation, with the assumption of constant specific heat at constant pressure for the fluid is:

$$\frac{\partial(\rho T)}{\partial t} + \frac{\partial(\rho uT)}{\partial x} + \frac{\partial(\rho vT)}{\partial y} = \frac{1}{c_p}\nabla.(k\nabla T) + \frac{\dot{q}_{\text{gen}}}{c_p}. \tag{6}$$

The flow is assumed to be incompressible, in what concerns the variation of density with pressure. Therefore, the variation of density of the fluid (air) with temperature can be determined from the following relation:

$$\rho T = \rho_\infty T_\infty. \tag{7}$$

The variation of the viscosity of air with temperature is determined from Sutherland's law [17] as follows:

$$\mu = 1.458 \times 10^{-6}\frac{T^{3/2}}{T + 110.4K}\left(\frac{\text{N.sec}}{\text{m}^2}\right). \tag{8}$$

The variation of specific heat at constant pressure, c_p and the Prandtl number, Pr, of air with temperature, is nearly negligible (the c_p and Pr of air, when the temperature varies between 300 K and 400 K, change 0.7% and 2.5%, respectively [18]). Therefore, c_p and Pr can be considered to have a constant value in the range of temperatures (300-380 K) for which the computations are carried out. Under this assumption, the thermal conductivity for air with temperature can be determined from the value of μ through the following relation:

$$k = \frac{c_p \mu}{\text{Pr}}. \tag{9}$$

BOUNDARY AND INITIAL CONDITIONS

The flow is assumed to be symmetric about a vertical plane passing through the axis of the heat source (Figure 1), therefore, only one half plane will be considered. The boundary conditions for the symmetry plane ($y = 0$) are as follows:

$$v = 0 \quad \text{and} \quad \frac{\partial u}{\partial y} = \frac{\partial T}{\partial y} = 0. \tag{10}$$

The other boundaries are located relatively far away from the heat source and the pressure is assumed to have a constant value. In this study, the relative pressure is taken as zero ($p_\infty = 0$). Two types of condition for the energy equation are used at the "far-field" boundaries. For the inflow regions, it is assumed:

$$T = T_\infty \quad \text{(inflow)}. \tag{11}$$

For the outflow regions to reach higher accuracy, the second-order and one sided finite difference approximation of the temperature derivative are used instead of the first derivative, namely:

$$\frac{\partial^2 T}{\partial n^2} = 0 \quad \text{(outflow)}, \tag{12}$$

where n is the direction perpendicular to the surface of the boundaries [19]. This kind of boundary condition allows the transfer of energy through the boundary by advection and diffusion.

The initial conditions for the velocity components and temperature are as follows:

$$u(x, y, 0) = v(x, y, 0) = 0, \quad T(x, y, 0) = T_\infty. \tag{13}$$

NUMERICAL METHOD

The governing equations are discretized by a control volume method, and the resulting set of algebraic equations is solved by the SIMPLE algorithm [12-14]. In the discretization of nonlinear convection terms, the second-order upwind is used.

The governing equations were discretized for non-uniform staggered grids, which reach their smallest value at the fluid-solid interface. The discretized equations for fluid and solid (line source) phases were solved simultaneously. The values of the components velocity in the solid phase are set to zero, by choice of suitable source terms in the discretized momentum equations [13]. To avoid eventual divergence in the iterative solution, the under-relaxation factors of $0.5, 0.5, 0.8$ and 0.8 were used for u, v, p and T, respectively.

The discretized governing equations are solved for three different computational domain sizes (0.1 m $\times$ 0.05 m, 0.13 m $\times$ 0.065 m and 0.15 m $\times$ 0.075 m), in which the maximum Grashof number, based on the heat input rate, is less than the critical Grashof number in all of the testes.

The convergence criterion for every time step, based on the maximum relative residual of the discretized equations, is chosen as 0.01. The maximum relative residual of the discretized equations, at every time step, is defined as the relative of the maximum residual for every variable in the computational domain, at each iterate, to the same value in the second iterate.

RESULTS AND DISCUSSION

The Grashof number, similarity parameters, stream function and non-dimensional temperature, were defined by Gebhart et al. as:

$$\mathrm{Gr} = \frac{g\beta x^3 (T_0 - T_\infty)}{\nu^2}, \tag{14}$$

$$\xi = \frac{y}{x}\sqrt[4]{\left(\frac{\mathrm{Gr}}{4}\right)},$$

$$\psi = 4\nu\sqrt[4]{\left(\frac{\mathrm{Gr}}{4}\right)} f(\xi),$$

$$h(\xi) = \frac{T - T_\infty}{T_0 - T\infty}. \tag{15}$$

As a first step in the assessment of the accuracy of the predictions, using the present numerical model, the results of f, f' and h, based on the definition of Gebhart et al. [3], were calculated for a time of about 200 seconds (when the steady state is reached), which are presented in Figure 2. In this figure, these results are compared with the similarity solution of Gebhart et al. [3] for the steady-state boundary layer equations. In the vicinity of the centerline ($\xi \leq 2$) of the plume, the comparison is very good, however, in the region far away from the centerline of the plume, the predicted results deviate from the solution of Gebhart et al. [3], especially for the f variable. This finding is not unexpected, since in the far field, the boundary layer equation assumptions do not apply and the similarity solution of Gebhart et al. [3] is not valid in this region. This is further corroborated by comparing the results for the variables f, f' and h. They are plotted for different heights away from the center of the heat source (x equals 4, 7 and 10 cm). The similarity solution of Gebhart et al. [3] is for the boundary layer equations with constant fluid properties, while, in the present numerical study, the momentum equation in the y direction is not neglected and the fluid properties are dependent upon the temperature, as described by Equations 7 to 9.

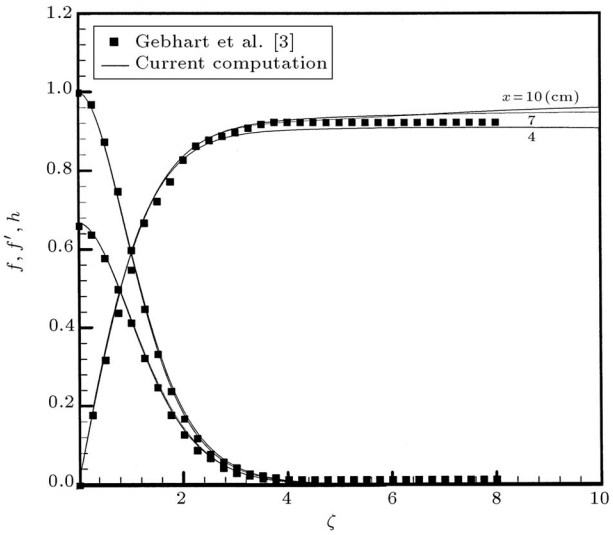

Figure 2. Comparison of the current computation with the results of Gebhart et al. [3] based on the boundary layer assumptions.

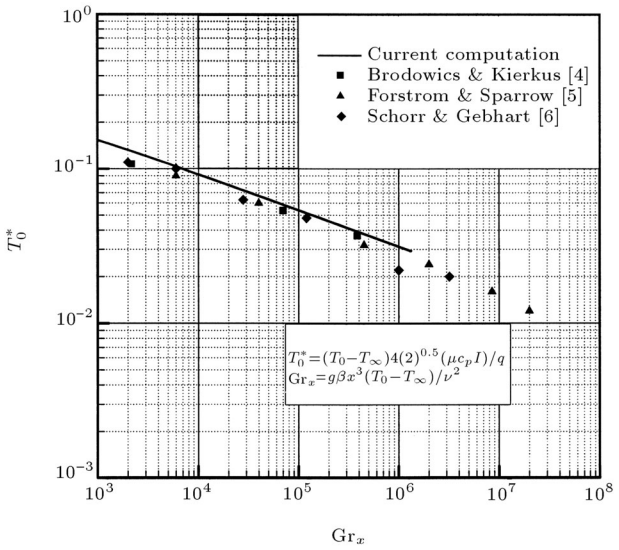

Figure 3. The variation of non-dimensional centerline temperature of thermal plume with respect to Grashof number.

The distribution of the centerline temperature in the x direction is an important variable characterizing the plume, as extensively discussed in the literature. Gebhart et al. [16] investigated the variation of the non-dimensional steady-state laminar centerline temperature of the plume, with respect to the Grashof number, for different experimental data. The non-dimensional centerline temperature of the plume is defined as:

$$T_0^* = (T_0 - T_\infty)4\sqrt{2}(\mu c_p I)/q, \tag{16}$$

where I depends only on the Prandtl number and is equal to 1.245 for Pr = 0.7 [16].

The present predictions for this quantity are compared in Figure 3 against the experimental results of Brodowics and Kierkus [4], Forstrom and Sparrow [5] and Schorr and Gebhart [6]. For all test cases, the experimental results described by T^* are about 10% lower than the present prediction. It should be mentioned that one of the parameters that causes major discrepancy between the experimental centerline temperature of the plume and the current predicted values, is the net radiation exchange between the surface of the heat source and its surrounding. In this study, it is assumed that the amount of this exchange is negligible and all of the input energy to the heat source is transferred through the fluid by diffusion and advection, while, in the experimental studies, part of the input energy to the heat source is transferred by radiation and the rest of it is transferred through the fluid by diffusion and advection, which is less than the input energy. Hence, this assumption causes the current computational results, to predict the centerline temperature of the plume, to be higher than the experimental ones.

The effect of computational domain size on the

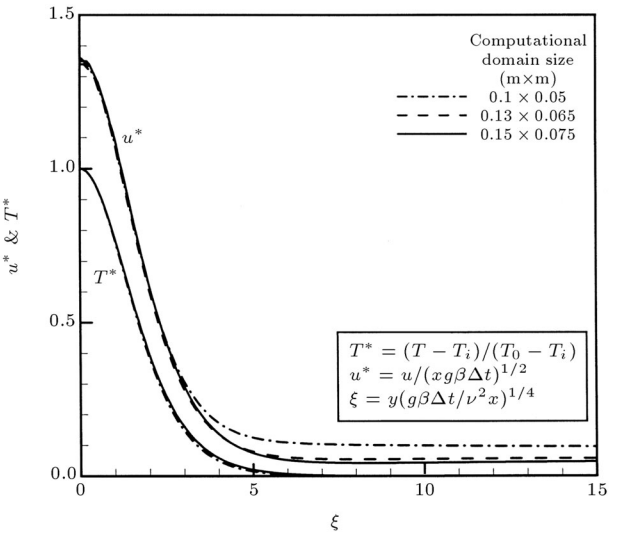

Figure 4. The effects of computational domain size on the results of u^* and T^*in the steady-state situation.

results of u^* and T^* are shown in Figure 4. For this purpose, the size of the computational domain is chosen to be 0.1 m × 0.05 m, 0.13 m × 0.065 m and 0.15 m × 0.075 m, respectively, which imposed the maximum Grashof number in all of the tests to be less than the critical Grashof number. This figure shows that the distribution of u^*, for the steady-state situation in the neighborhood of the centerline, is independent of the computational domain size. For the size bigger than 0.13 m×0.065 m, this value is independent in the whole domain. Also, the T^* distribution is less sensitive to the computational domain size than the u^*.

The mesh convergence of the results was also carefully analyzed. The effect of mesh size on the results of u^* and T^* are shown in Figure 5. For this

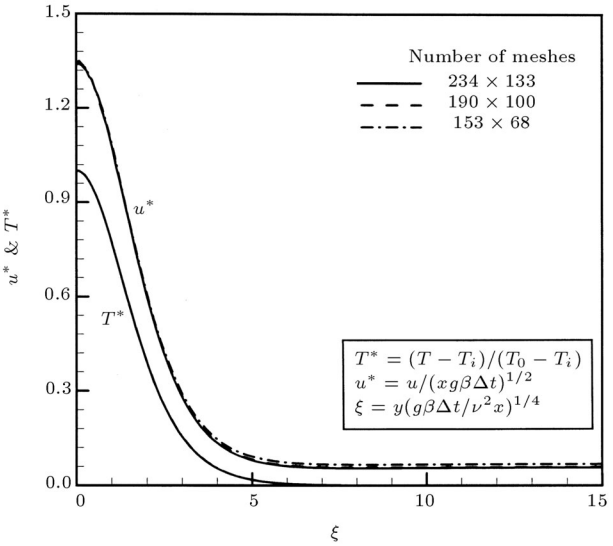

Figure 5. The effects of mesh size on the results of u^* and T^* in the steady-state situation.

purpose, the number of the meshes is chosen as being $153 \times 68, 190 \times 100$ and 234×133, respectively. This figure shows that the distribution of u^* and T^* for the steady-state situation, with respect to non-dimensional time in the computational domain, are, approximately, independent of mesh size for mesh numbers higher than 190×100. Figure 5, also, shows that the distribution of T^* in the computational domain is less sensitive to the mesh size than the distribution of u^* on the same region.

The variation of non-dimensional heat transfer from the solid boundary to the surrounding fluid and from the boundary of the computational domain, with respect to non-dimensional time, is shown in Figure 6. This figure shows that heat is transferred from the

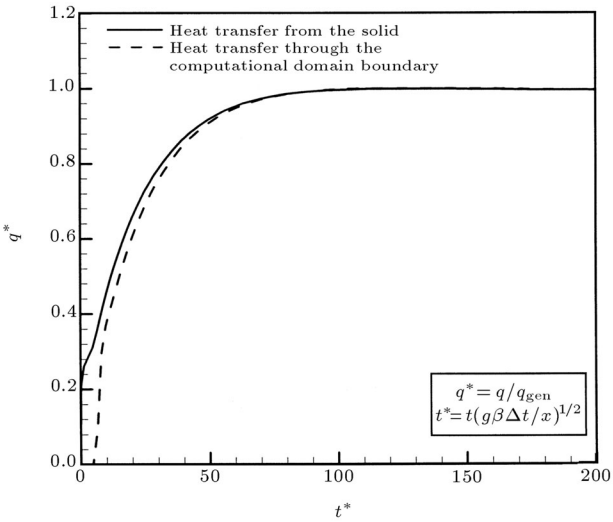

Figure 6. The variation of the non-dimensional heat transfer from the solid boundary and from the boundary of the computational domain versus non-dimensional time.

solid to the fluid from the beginning of the process, but there is no heat transfer from the boundary of the computational domain up to t^* equals about 5. The energy that is transferred to the fluid during this time is stored in the fluid, which causes its temperature to increase. After this time, heat transfer by advection and conduction takes place across the boundary of the computational domain and it progresses with time.

A typical present prediction for the history of streamlines and isotherms in the solid and fluid field, from 0.2 s to 180 s, is reported in Figure 7. The energy source has a volumetric generation of 10^7 W/m^3 and its dimensions are 0.1 cm by 0.1 cm, which equals the heat generation amount (10 W/m) that is used by Brodowicz and Kierkus [4] in their experimental studies. In the early stages of the transient process ($t < 2$ sec), heat is transferred by pure conduction through the fluid field. Hence, there are no obvious changes in the streamlines and the isotherms around the solid take a circular shape. Beyond 2 seconds, however, a mode transition sets in by the convective effects and the fluid around the solid starts rising. The recirculating eddies that form around the solid move upward and this motion causes the shape of the isotherms to change from a circular to elliptic shape. This process is continued until the eddies reach the top boundary of the computational domain at a time approximately equal to 8 seconds. During this process, eddies do grow and the heat transfer front progresses at a faster rate than that of early times. From 50 seconds to 180 seconds, the shape of the streamlines and the shape of the isotherms are similar and present no obvious changes. This is an indication that the process has reached steady state. Beyond 8 seconds, the streamlines near the centerline of the plume get narrower as time evolves. This means that the velocity in the vicinity of the centerline of the plume is increasing with respect to time.

The results of the present study for the shape of streamlines at about 180 seconds (steady-state) are similar to the experimental results of Brodowicz and Kierkus [4]. These authors measured velocity and temperature in the free convection flow field above a horizontal wire in air, with constant heat generation in the wire under a steady-state condition.

Figure 8 shows the variation of the non-dimensional maximum temperature in solid versus non-dimensional time. In the early stages of the transient development, heat is transferred from the solid to the fluid by pure conduction and, since the thermal conductivity of the air is low ($k < 1$ W/m.K), most of the energy generated in the solid is to be stored in it. Therefore, this condition yields a very rapid increase of the solid temperature. Further on in the transient development, the flow field is established and

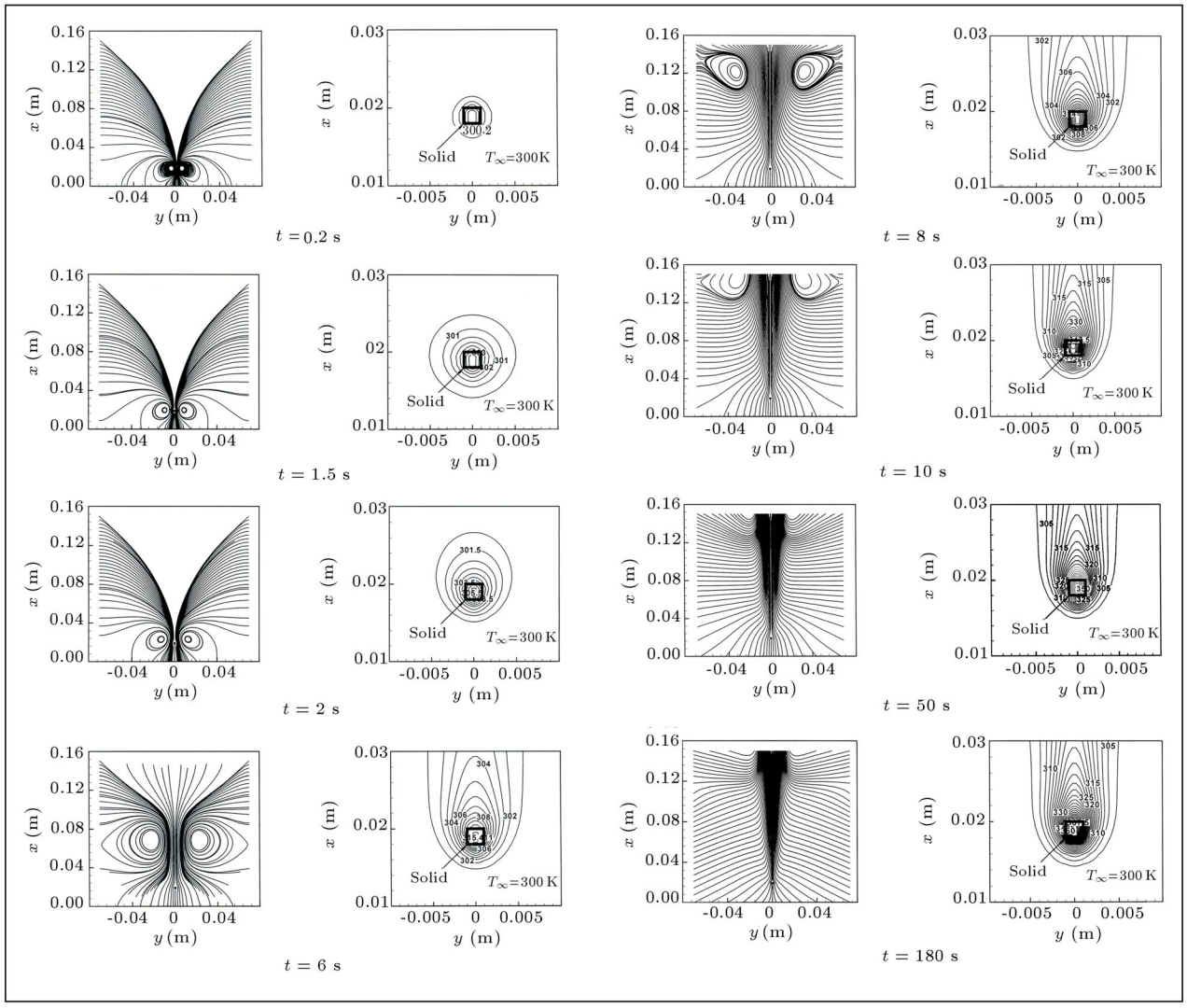

Figure 7. The variation of the streamlines (left side) and the isotherm (right side) ($q = 10$ W/m).

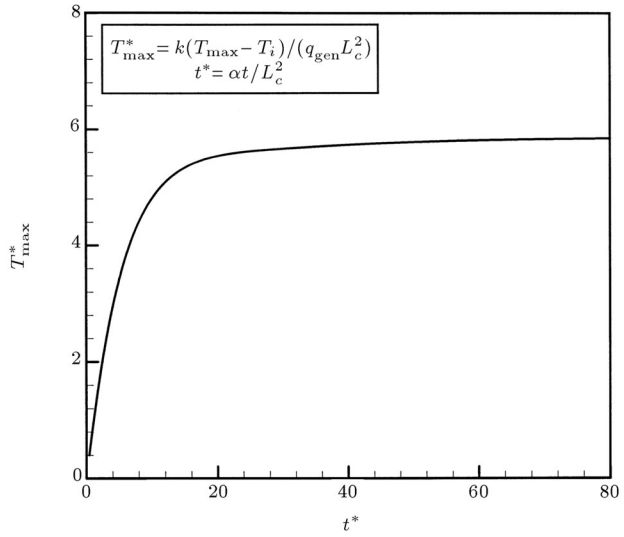

Figure 8. The variation of non-dimensional maximum temperature in the solid versus non-dimensional time.

heat transfer by advection becomes dominant. This causes a reduction in the rate of change of the solid temperature until steady-state is reached, when the solid temperature attains a constant value.

The distribution of non-dimensional temperature in the fluid, for six different non-dimensional times ($t^* = 4.7, 6.5, 8, 13, 160$ and 322), is shown in Figure 9. This figure shows that there is not an obvious change in the non-dimensional temperature of the fluid in the computational domain beyond t^* equals, about, 13.

The distribution of the non-dimensional vertical component of velocity, (u^*), in the fluid field for six different non-dimensional times ($t^* = 0.002, 1.26, 4.7, 25, 160$ and 322), is shown in Figure 10. The vertical components of velocity in the fluid field in the vicinity of the center line of the plume reach steady-state at t^* equals, about, 25, but it varies beyond this time in the far field. With a comparison of Figures 9 and 10, one concludes that temperature distribution

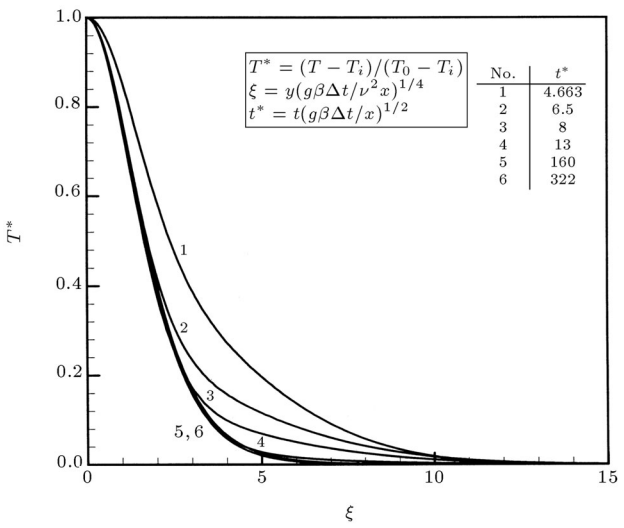

Figure 9. The distribution of non-dimensional fluid temperature at six different non-dimensional times.

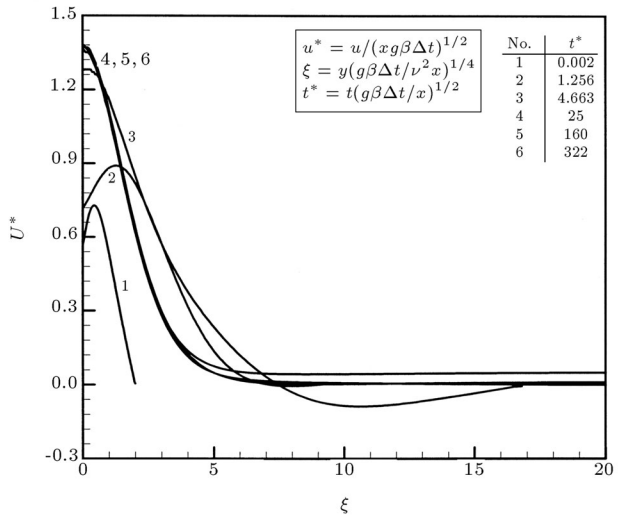

Figure 10. The distribution of u^* (non-dimensional vertical component of velocity) in the fluid at six non-dimensional different times.

in the computational domain reaches to a steady-state situation earlier than velocity distribution in the same region.

CONCLUSION

In this study, the analysis of a transient, two-dimensional, laminar thermal plume, induced by a horizontal line heat source, is conducted by using numerical techniques associated with the SIMPLE method. The computational results are presented for a time range of between 0 and 180 seconds.

The transient numerical procedure, over time, yields a steady-state solution, which is in good agreement with the steady-state, self-similar results of Gebhart et al. [3].

In the early time stages, heat is transferred by pure conduction, while the solid temperature increases very rapidly and the isotherms in the fluid region present a circular shape. But, beyond 2 seconds, flow takes place and heat is, simultaneously, transferred by advection and conduction through the fluid (air). As time goes on, the contribution of the advection mode increases, which causes the rate change of the solid temperature to decrease.

The numerical results show that the temperature distribution in the fluid reaches steady-state earlier than the velocity distribution, in particular for the far field region with respect to the solid.

The distribution of temperature in the computational domain is less sensitive to the mesh size and the computational domain size than the velocity distribution in the same region.

NOMENCLATURE

c_p	specific heat
f	dimensionless stream function
g	gravitational acceleration
Gr	Grashof number
h	dimensionless temperature
H	height of computational domain
k	thermal conductivity
p	pressure
Pr	Prandtl number
q'_{gen}	heat generation
q	heat transfer rate per unit length
T	temperature
t	time
u	velocity component in the x direction
v	velocity component in the y direction
V	velocity vector
x	coordinate along vertical direction
X	body force in the x direction
y	coordinate along horizontal direction
W	width of computational domain

Greek Symbols

β	thermal expansion coefficient
μ	dynamic viscosity
ν	kinematics viscosity
ρ	density
σ	normal stress
τ	shear stress
ξ	similarity variable
ψ	stream function

Superscripts

$*$	non-dimensional variables

Subscripts

i	initial condition
∞	ambient

REFERENCES

1. Zeldovich, Y.B. "Limiting laws of freely rising convection currents", *Zh. Eksp. Teor. Fiz.*, **7**, pp 1463-1465 (1937).
2. Fujii, T. "Theory of the steady laminar natural convection above a horizontal line heat source and a point heat source", *Int. J. Heat Mass Transfer*, **6**, pp 597-606 (1963).
3. Gebhart, B., Pera, L. and Schorr, A.W. "Steady laminar convection plumes above a horizontal line heat source", *Int. J. Heat Mass Transfer*, **13**, pp 161-171 (1970).
4. Brodowicz, K. and Kierkus, W.T. "Experimental investigation of laminar free convection flow in air above horizontal wire with constant heat flux", *Int. J. Heat Mass Transfer*, **9**, pp 81-94 (1966).
5. Forstrom, R.J. and Sparrow, E.M. "Experiments on the buoyant plume above a heated horizontal wire", *Int. J. Heat Mass Transfer*, **10**, pp 321-331 (1967).
6. Schorr, A.W. and Gebhart, B. "An experimental investigation of natural convection wakes above a line heat source", *Int. J. Heat Mass Transfer*, **13**, pp 557-571 (1970).
7. Linan, B.A. and Kurdymov, V.N. "Laminar free convection induced by a line heat source, and heat transfer from wires at small Grashof numbers", *J. Fluid Mech*, **362**, pp 199-227 (1998).
8. Katagiri, M. and Pop, I. "Transient free convection from an isothermal horizontal circular cylinder", *Wärme-und Stoffübertr*, **12**, pp 73-81 (1979).
9. Sako, M., Chiba, T., Garza, J.M.S. and Yanagida, A. "Numerical solution of transient natural convection heat transfer from a horizontal cylinder", *Jap. Heat Transfer*, **11**, pp 24-44 (1982).
10. Shin, S.C. and Chang, K.S. "Transient natural convection heat transfer from a horizontal circular cylinder", *Int. Comm. Heat Mass Transfer*, **16**, pp 803-810 (1989).
11. Wang, P., Kahawita, R. and Nguyen, D.L. "Transient laminar natural convection from horizontal cylinders", *Int. J. Heat Mass Transfer*, **34**, pp 1429-1442 (1991).
12. Esfahani, J.E. and Sousa, A.C.M. "Ignition of epoxy by a high radiation source. A numerical study", *Int. J. Thermal Science*, **38**, pp 315-323 (1999).
13. Patankar, S.V., *Numerical Heat Transfer and Fluid Flow*, McGraw-Hill (1980).
14. Van Doormaal, J.P. and Raithby, G.D. "Enhancements of the SIMPLE method for predicting incompressible fluid flows", *Numerical Heat Transfer*, **7**, pp 147-163 (1984).
15. Thakur, S. and Shyy, W. "Some implementational issues of convection schemes for finite-volume formulations", *Numerical Heat Transfer*, Part B, **24**, pp 31-55 (1993).
16. Gebhart, B., Jaluria, Y., Mahajan, R.L. and Sammakia, B., *Buoyancy Induced Flows and Transport*, Hemisphere Publishing Corporation, New York, USA (1988).
17. Anderson Jr., J.D., *Fundamentals of Aerodynamics*, 2nd Ed., Mac Graw-Hill, New York, USA (1991).
18. Incropera, F.P. and DeWitt, D.P., *Fundamentals of Heat and Mass Transfer*, 5th Ed., John Wiley & Sons, New York, USA (2002).
19. Ferziger, J.H. and Peric, M., *Computational Methods for Fluid Dynamics*, Springer, Germany (1997).